

AR-5 1193



1  
2  
3  
4

PROPOSED TRAVELLING WAVE TUNNETT AMPLIFIER AND  
OSCILLATOR FOR AIRBORNE RADARS

HOSNY A. EL-MOTAAFY \*

ABSTRACT

Two travelling wave TUNNETT diode structures are proposed. The first one is a distributed TUNNETT which is proposed in order to overcome the inherent limitations on the power output of the discrete TUNNETT structure. It is shown that this structure can be used as resonant lengths of transmission line in order to tune out the diode depletion layer capacitance. Therefore, the distributed structure can have a much higher impedance, a larger area and a higher output power than the discrete one and will be much easier to match. It is found that a relatively high substrate resistivity gives better performance. It is also found that for a given substrate resistivity there is an optimum value of substrate thickness. Design graphs for the proposed device are presented. An output power of about 12 watts has been obtained at a frequency of 30 GHz which is an important result. The second proposed structure is a multistream TUNNETT structure which is based on the space charge interactions of electron streaming layers. Each layer has a different average velocity due to a properly chosen concentration gradient along the direction transverse to the motion of electrons. A numerical analysis is used to determine the gain of the proposed structure when it is used as a travelling wave amplifier. It is found that this gain decreases with increasing the diode thickness and slightly increases with the operating frequency in the frequency range considered. The proposed devices suffer no transit-time limitations so their bandwidth is much wider than that of a discrete TUNNETT. The possible applications of the proposed devices in airborne radars are indicated.

---

\* Ph.D , Department of Radar, Military Technical College, Cairo, Egypt.

## I. INTRODUCTION

Microwave power may be generated by a transit-time diode in reverse breakdown from either the avalanche mechanism, a tunnel mechanism or a mixed avalanche-tunnel mechanism [ 1 ]. The breakdown is avalanche dominated for low electric fields ( 500 KV/cm ) and tunnel dominated for high electric fields ( 1 MV/cm ). Three distinct modes of operation are identified for different widths of the generation region [ 2 ]. These include the normal IMPATT mode, the MITATT (mixed tunnelling and avalanche transit time ) mode where both tunnelling and avalanche breakdown exist, and the TUNNETT ( tunnel transit time ) mode where pure tunnelling is present. The TUNNETT mode is characterized by the injected current pulse being approximately in phase with the RF voltage wave, which results in the device negative conductance being caused only by transit time effects. The TUNNETT mode has a lower RF power than the IMPATT mode but the TUNNETT noise level is much smaller since no avalanche generation is involved. The MITATT mode exhibits a noise performance-output power tradeoff. It is not generally possible to increase the output power through increasing the device area because the device negative resistance will be reduced to a level comparable with circuit losses. Therefore, efficiency will be markedly reduced and eventually oscillation conditions will not be achieved. However, if the device capacitance could be shunt resonated at the depletion-layer terminals so as to leave only the negative conductance of the active region, then much larger area devices could be used. The present paper shows how this might be achieved using a large area TUNNETT structure made as a resonant length of transmission line. The distributed TUNNETT diode shown in Fig.1 is proposed. Obviously many other doping profiles rather than the p-n-p profile can be used too. In the structure shown, the electrons propagate in the x-direction while the wave propagates in the z-direction. Another structure is proposed and is expected to give a very wide bandwidth; it will be referred to as the multistream TUNNETT structure. In this structure, the wave to be amplified co-propagates with the electron beam ( e.b ) in the same direction. In the following sections, the performance of the proposed devices will be analyzed.

## II. THE PROPOSED DISTRIBUTED TUNNETT STRUCTURE

The proposed distributed TUNNETT structure is shown in Fig.1. It is assumed that the width  $w$  is large compared with the total thickness (  $b + d$  ) of the depletion and substrate regions so that the effect of fringing field on the wave propagation is negligible. In the depletion region, the RF electric field is essentially in the direction of carrier drift. There is an axial component of electric field but it is much smaller than the transverse field. The substrate region is generally of sufficiently low resistivity. Solving the semiconductor transport equations under small signal conditions as it is described elsewhere [ 3 ] we can study the effects of the parameters characterizing the proposed structure such as the substrate thickness  $d$  and the substrate resistivity  $r$  on the output parameters. The shunt conductance  $G_d$  and the shunt susceptance  $B_d$  can be obtained from the small-signal theory of the TUNNETT [ 4 ]. It is obvious that for proper operation  $G_d$  should be negative at the operating frequency.

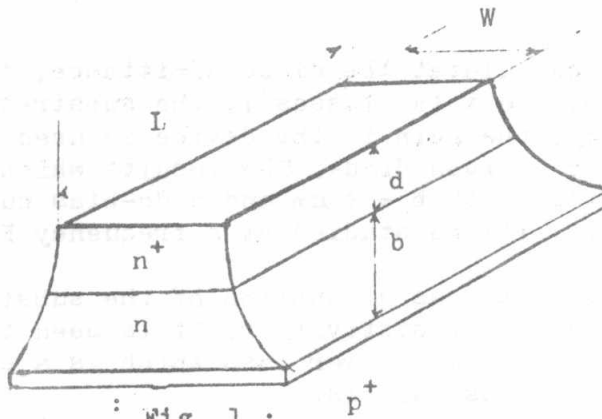


Fig. 1 :

The proposed distributed travelling-wave TUNNETT diode.

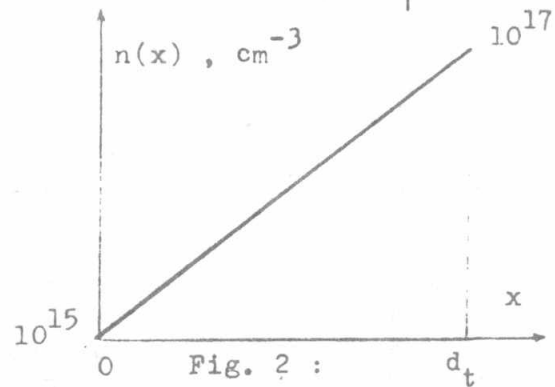
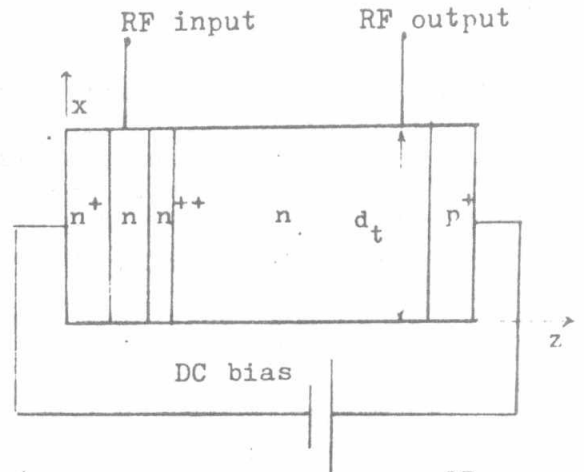


Fig. 2 :

The proposed multistream TUNNETT diode and its doping density in the transverse direction x.

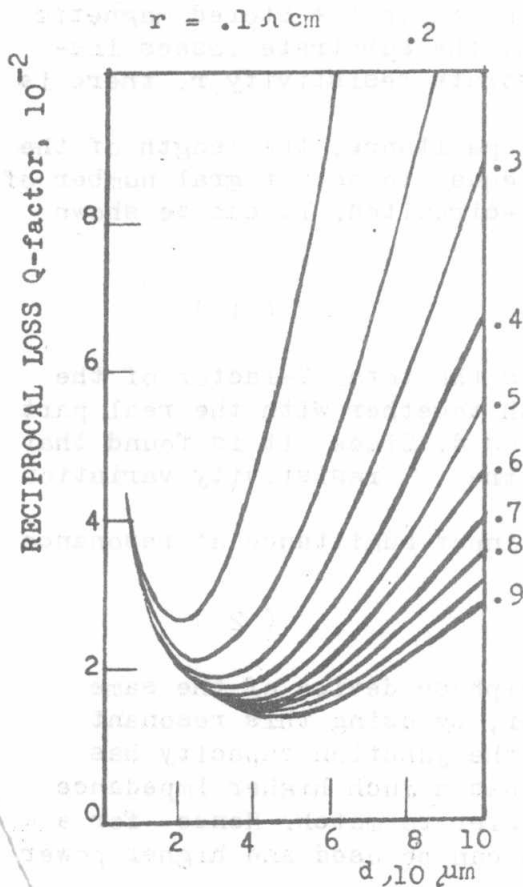


Fig. 3 : The reciprocal loss Q-factor vs. the substrate thickness.

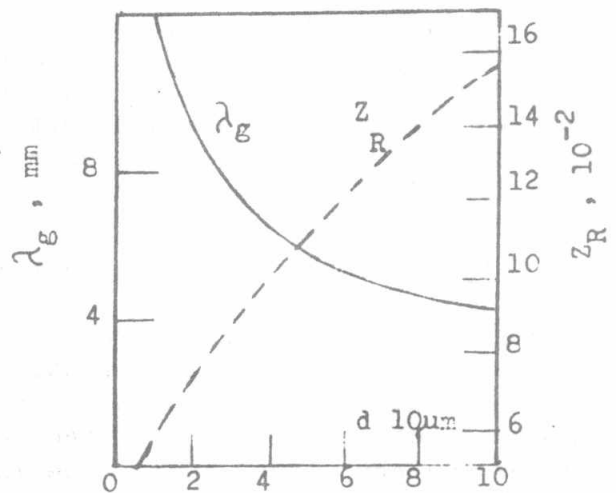


Fig. 4 : The guide wavelength  $\lambda_g$  and the real part of the characteristic impedance vs. d.

A computer program is written to calculate the diode admittance, the wavelength of the travelling wave, the total losses in the substrate and conductor, the transfer efficiency, the gain if the device is used as an amplifier and the output power for a given diode. The results which will be presented here are for a Si diode with  $b = 2 \mu\text{m}$  and a dc-bias current  $J_{dc} = 1000 \text{ A/cm}^2$ . The performance will be studied at a frequency  $F = 30 \text{ GHz}$ .

Fig.3 shows the reciprocal loss Q factor as a function of the substrate thickness  $d$  for different values of the resistivity  $r$ . It is seen that for a given  $d$ , a higher resistivity gives a lower loss which is a surprising result. This can be explained as follows:

In the distributed TUNNETT, the electric field in the substrate is predominantly longitudinal; that is parallel to the plane of the junction and in the direction of wave propagation. Since we are concerned with substrate thickness in general small compared with the skin depth, the magnitude of the longitudinal electric field will only change slowly with substrate resistivity. Hence, increasing the resistivity will result in smaller longitudinal currents and reduced substrate dissipation. It is also seen that the reciprocal Q-factor has a minimum at a value of  $d$  which increases with the substrate resistivity. This is because the effect of conductor losses decrease with increasing  $d$  since the dissipation remains essentially constant while the stored magnetic energy increases with  $d$ . On the other hand, the substrate losses increase with  $d$ . Therefore, for a given substrate resistivity  $r$ , there is an optimum substrate thickness.

In order to tune out the depletion-layer capacitance, the length of the distributed TUNNETT must be approximately equal to an integral number of half guide wavelengths if one end is open-circuited. It can be shown that this length is given by :

$$L = n \lambda_g ( 1 - 1/4 Q_t^2 ) / 2 \quad ( 1 )$$

where  $\lambda_g$  is the guide wavelength and  $Q_t$  is the total Q-factor of the structure. Fig.4 shows the guide wavelength together with the real part of the diode characteristic impedance versus  $d$ . Since it is found that these two parameters are not sensitive to the resistivity variation they are drawn only for  $r = 0.4 \Omega \text{ cm}$ .

If the losses are assumed to be zero, the input admittance at resonance is given by :

$$Y_{in} = G_d L / 2 \quad \text{mho/unit width} \quad ( 2 )$$

This value is only one half that of an equiphase device of the same area biased at the same dc current. However, by using this resonant mode of operation, the shunting effect of the junction capacity has been tuned out and the distributed device has a much higher impedance than the equiphase one and will be much easier to match. Hence for a given circuit impedance, much larger areas can be used and higher power obtained.

Fig.5 shows the transfer efficiency versus  $d$  for different values of  $r$ . The transfer efficiency is the ratio of the maximum output power available to that available if the substrate and conductor losses were zero. It is seen that the efficiency increases with  $r$ . This is because as it is already indicated-, the reciprocal loss Q-factor decreases with

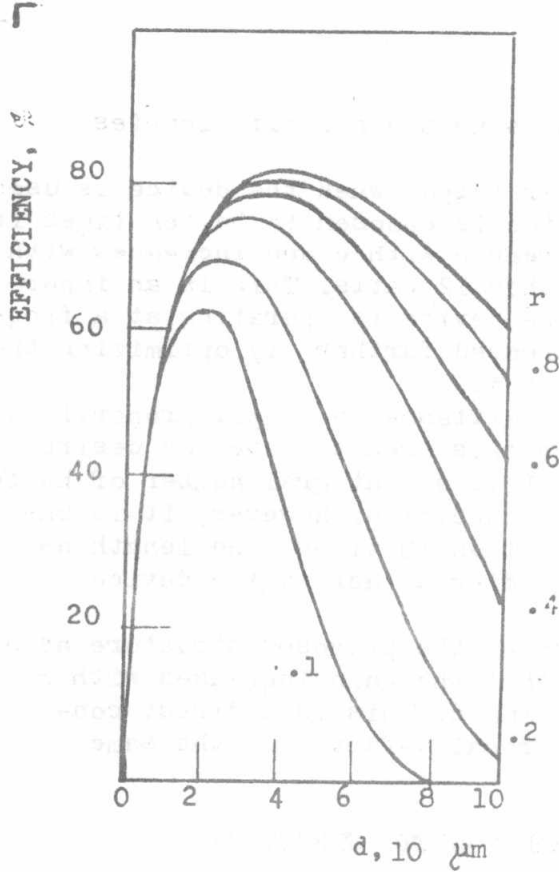


Fig. 5 : The transfer efficiency vs. d.

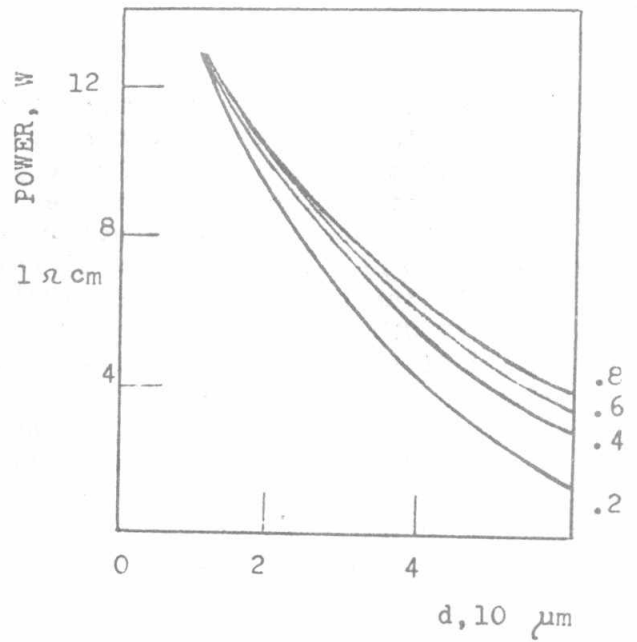


Fig. 6 : The power output vs. the substrate thickness d, for different values of substrate resistivity.

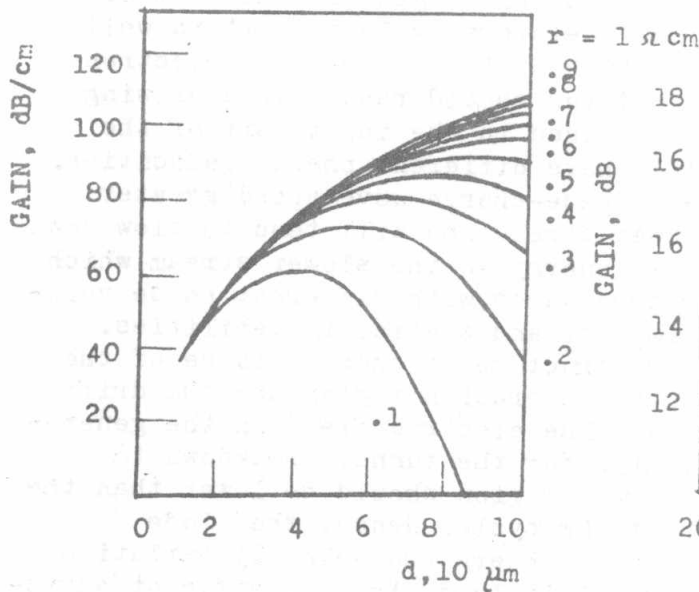


Fig. 7 : The gain vs. the substrate thickness.

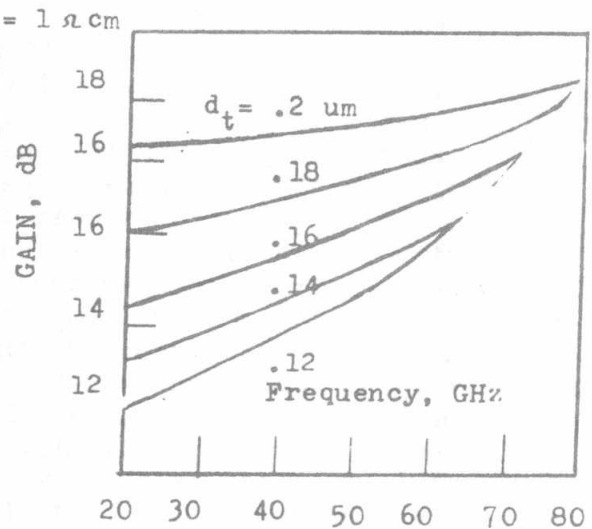


Fig. 8 : The gain of the multi-stream TUNNETT diode vs. the frequency.

r. It is also seen that by properly choosing  $d$  and  $r$ , efficiencies higher than 70 % could be obtained.

Fig. 6 shows the maximum available power output when the device is used as an oscillator. The width of the device is chosen to be ten times its length. It is seen that this power decreases with  $d$  and increases with  $r$ . For  $d = 10 \mu\text{m}$  the power is higher than 12 watts. This is an important result taking into account that the device is operating at a frequency of 30 GHz. This value can be increased further by optimizing the doping profile and the operating conditions.

For the proposed structure, the input admittance is simply proportional to the device area  $w \times L$ . We can choose this area to give any desired value of input impedance provided that  $L$  is an integral number of half-wavelength as required by the resonance condition. However, it is undesirable to have the device width more than 10 times the length as this would undoubtedly lead to modes building up across the device instead of along it.

Fig. 7 shows the gain in the case of using the proposed structure as a travelling wave amplifier. It is seen that the gain increases with  $r$  and that for a given  $r$  there is an optimum  $d$ . This is a direct consequence of the dependence of the reciprocal  $Q$ -factor on the same parameters as it is already indicated.

### III. THE PROPOSED MULTISTREAM TUNNETT STRUCTURE

The proposed multistream TUNNETT structure is shown in Fig. 2. This device is characterized by non-uniform doping densities along the semiconductor transverse direction  $x$ . The electric field is applied along the device length in the  $z$  direction. As a result, the electrons generated by the tunnelling breakdown mechanism and injected into the drift region will move through this region in the form of many layers with slightly different dc-lateral velocity. It is well known that the space charge interaction of two homogeneous electron streams of slightly different velocities should result in a growing wave. When a small RF field is introduced in the input port of the device, the space charge waves will have different phase velocities. A high velocity stream will have a space-charge wave speed greater than that of the neighbouring slower stream and will tend to slow down by transferring part of its kinetic energy to the slower stream which tends to speed up. Thus, space-charge waves with different phase velocities will interact and cause temporal and spatial instabilities. The doping profile of the proposed structure is chosen to be of the low-high-low type. Consequently, the generation region and the drift region can be optimized separately. The electric field in the generation region must be sufficiently high for the tunnel breakdown to occur. The electric field in the drift region should be lower than the saturation field during the complete RF cycle. Hence, the diode operates in the low field region where the velocity variation with the doping density is greatest. This leads to a significant advantage over conventional solid-state amplifiers, i.e., the operation is of the low-field and low-current type, so excessive Joule heating can be avoided; thus allowing CW instead of pulse operation. We propose to fabricate the diode using the GaAs material because its low-field mobility is very high.

Maxwell's equations together with the current density and continuity equations are solved numerically under small-signal conditions to determine the gain of the proposed device. The doping density in the drift region is assumed to vary linearly along the transverse direction  $x$ . Fig. 8 shows the gain as a function of frequency for different values of diode thickness. It is seen that the gain increases with decreasing the diode thickness and with increasing the operating frequency. This result indicates that the proposed device can be used as a very broad-band amplifier and this is expected because the proposed device is free from transit time limitations.

#### IV. APPLICATIONS OF THE PROPOSED DEVICES TO AIRBORNE RADARS

The proposed devices would be useful as low-noise wide-band amplifiers, medium power oscillators, self-oscillating mixers and detectors particularly at millimeter and submillimeter wavelengths. Therefore, these devices can have many wide applications in airborne multifunction radars, in radar altimeters, in electronic scanning radars, in solid-state Doppler radars and in airborne electronic countermeasures equipments especially as the active element in barrage jammers due to its large bandwidth. Fig. 9 shows the block diagram of a pulse compression radar using the proposed device. Fig. 10 shows a block diagram of an airborne frequency agile radar using also the proposed devices. In order to reduce the size of the antenna used in these airborne radars it is advantageous to operate at millimeter wavelengths. This requirement is satisfied using the proposed devices with a reasonable power and efficiency as it is indicated.

#### CONCLUSIONS

In this paper, two travelling wave TUNNETT diode structures are proposed. The first one is a distributed structure in which the velocity vectors of the electrons are orthogonal to the direction of wave propagation. It is found that a relatively high resistivity substrate gives better efficiency. It is also found that for a given resistivity there is an optimum substrate thickness. It is indicated that for a given value of circuit impedance, the proposed structure can be much larger in area and output power than the corresponding discrete TUNNETT. This is because the depletion-layer capacitance has been tuned out by properly choosing the diode length. A power output higher than 12 watts is obtained at a frequency of 30 GHz which is an important result. The second proposed structure is a multistream TUNNETT diode where the doping density varies linearly along the transverse direction in the drift region. In this device, the wave propagates in the same direction as the electron streams. Since this device is also a distributed structure, it is free from transit time limitations and it has a very wide bandwidth. It is found that its gain increases with decreasing the diode thickness and increasing the operating frequency.

#### REFERENCES

1. M. E. Elta and G. I. Haddad, "Large-signal performance of microwave transit-time devices in mixed tunnelling and avalanche breakdown," IEEE Trans. Electron Devices, vol. ED-26, June, 1979.
2. M. E. Elta and G. I. Haddad, "High-frequency limitations of IMPATT, MITATT, and TUNNETT mode devices," IEEE Trans. Microwave Theory Tech. vol. MTT-27, no. 5, May, 1979.
3. H. A. El-Motaafy, "Proposed travelling wave BARITT amplifier and oscillator," Fourth National Radio Science Symposium, 1986, Cairo, Egypt.
4. M. E. Elta, "The effects of mixed tunnelling and avalanche breakdown on microwave transit-time diodes," Tech. Report 142, Electron Physics Laboratory, Univ. of Michigan, Ann Arbor, June, 1978.

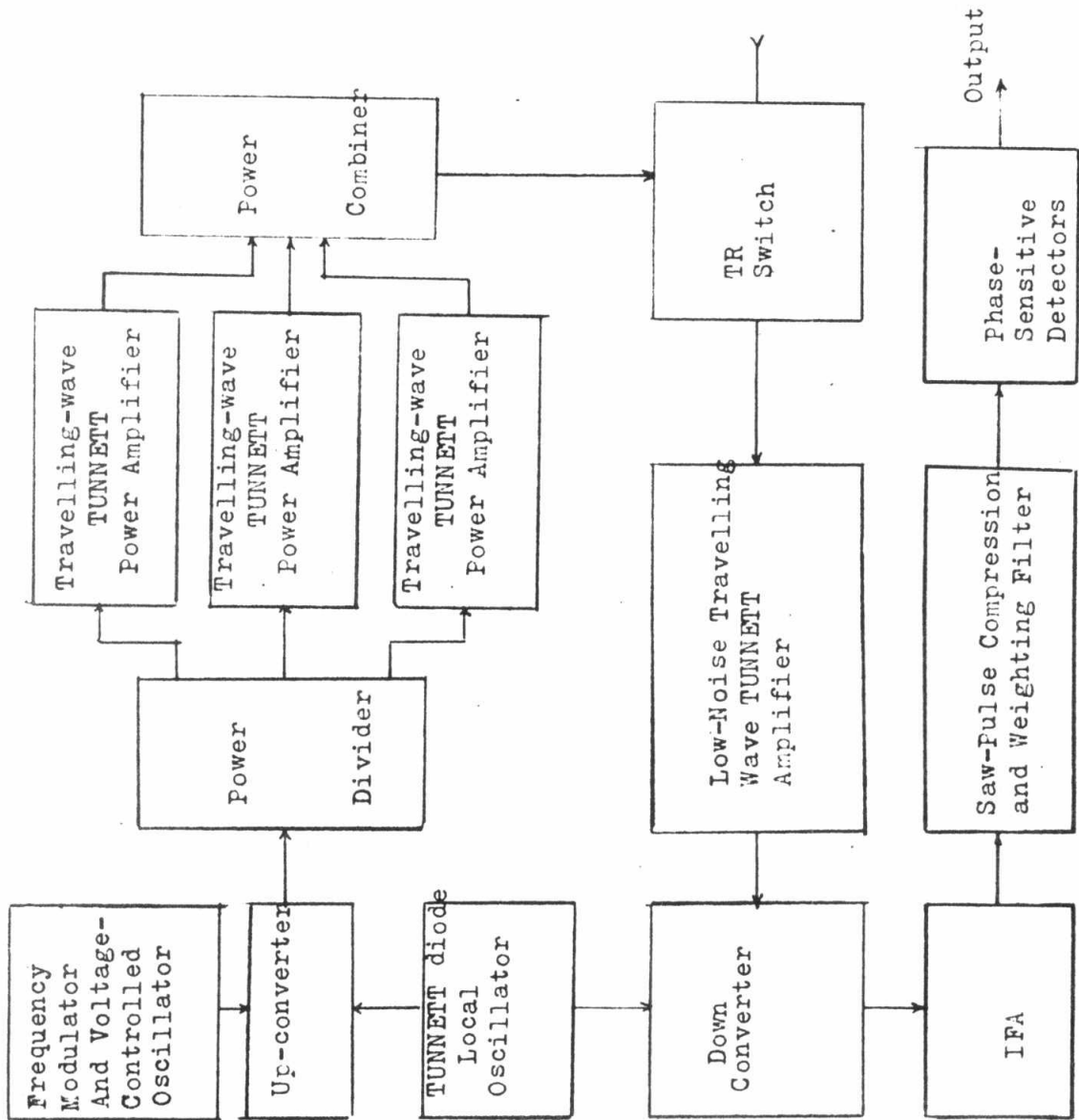


Fig. 9 : Block diagram of an airborne pulse compression radar using the proposed travelling-wave TUNNETT diode

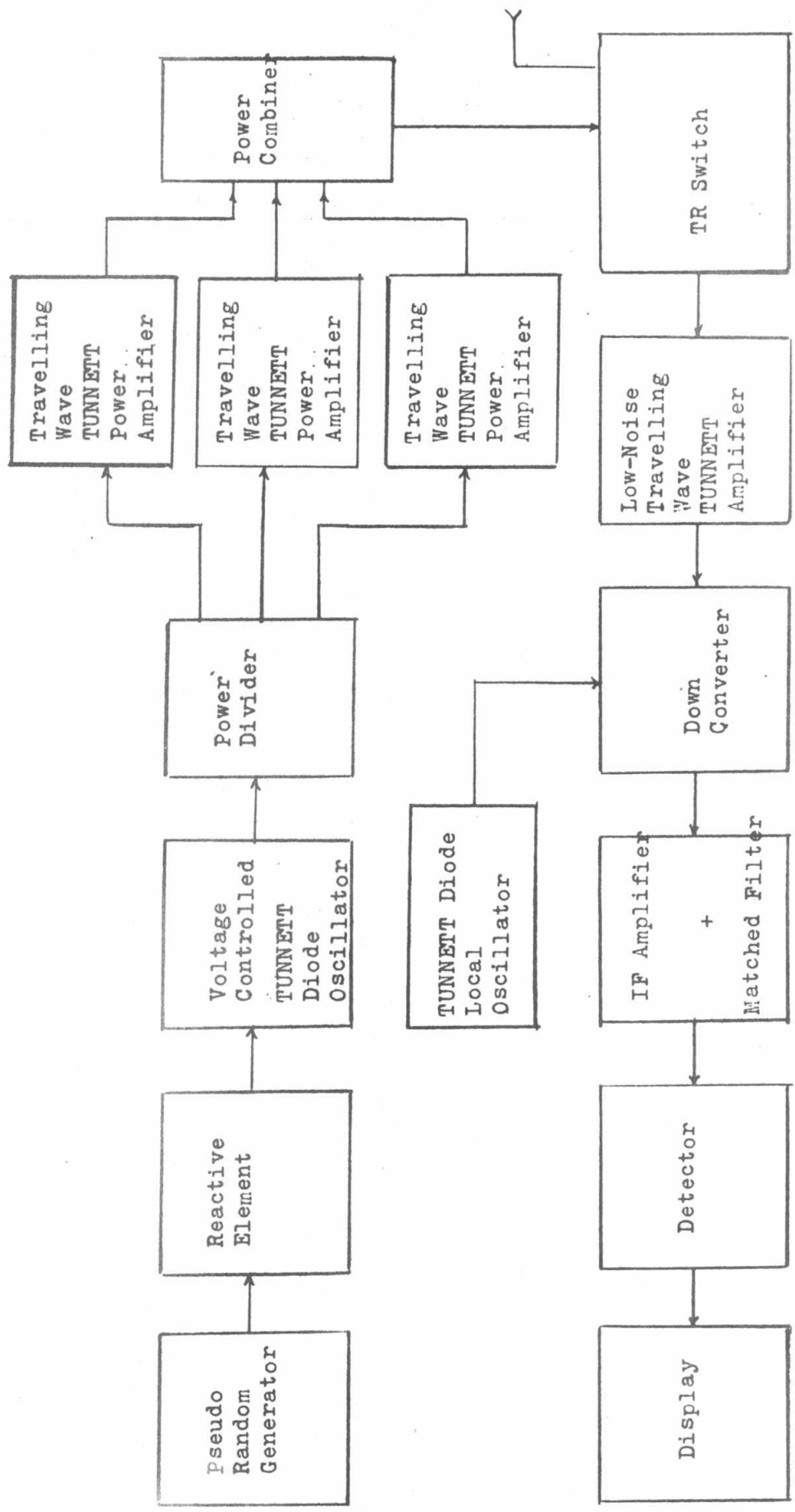


Fig. 1C : Block diagram of an airborne frequency agile radar using the proposed travelling-wave TUNNETT diode.